YERBİLİMLERİ
Bulletin for Earth Sciences
ISSN: 2687 - 2978
Yerbilimleri, 2019, 40 (3), 234-252, DOI: 10.17824/yerbilimleri.579538
Hacettepe Üniversitesi Yerbilimleri Uygulama ve Araştırma Merkezi Bülteni
Bulletin of the Earth Sciences Application and Research Centre of Hacettepe University

Kabuk Anizotropi Araştırmalarında Deprem Kümelerinin İstatistiksel Analizi

Statistical Analysis of the Earthquake Swarms in Crustal Anisotropic Investigations

GÜLTEN POLAT [1, *]

[1] *Department of Civil Engineering, Yeditepe University, 26 Ağustos Yerleşkesi, Kayışdağı Cad. 34755, Istanbul, Turkey*

Geliş (received): 18 Haziran (June) 2019
Kabul (accepted) : 5 Aralık (December) 2019

ABSTRACT

The seismic activity of the Simav region is very high so that swarm earthquakes usually occur in this region. Such swarms were usually convenient to measure crustal anisotropy by using shear wave splitting method. Therefore, the swarms make possible to detect crustal anisotropy beneath the study area. In addition, seismic b-value and stress were investigated by using the frequency–magnitude relationship of earthquakes as a function of space in order to find out whether a possible relationship between seismic anisotropy and seismic b-value is or not. For seismic b-value, an earthquake catalog prepared by the KOERI (Bogazici University, Kandilli Observatory and Earthquake Research Institute, Regional Earthquake-Tsunami Monitoring Center) with magnitude greater than 1.0 from 1 January 2010 to 28 February 2019 was used. Hence, the reliability of findings obtained from the analysis was improved because correctly determining location parameters of earthquakes before 2010 for this region is not reliable due to a lack of seismic station coverage. For splitting analysis, micro-earthquakes from 2016 to 2017 occurred in this region were initially selected. Results from shear wave splitting analysis indicated strong scattering in splitting parameters. This observation seems to be consistent with stress accumulation caused by the earthquake swarms. Additionally, due to variations in stress, changes in the average time-delay for each station were observed. Another important observation of the study is that 90°-flips in shear-wave polarizations observed. Fluctuating high pore-fluid pressures on seismically active fault planes are the most likely cause of the scattering pattern in shear wave splitting parameters.

Keywords: Simav, seismic anisotropy, shear wave splitting, stress, b-value, and seismic hazard.

---

https://doi.org/10.17824/yerbilimleri.579538

Gülten POLAT gultenpolat2005@gmail.com

[1] *Dep. of Civil Engineering, Yeditepe Univ., 26 Ağustos Yer., Kayışdağı Cad. 34755, Istanbul, Turkey, ORCID* 0000-0002-6956-7385

ÖZ

Simav bölgesinin sismik aktivitesi çok yüksektir, bu nedenle genellikle bu bölgede küme depremleri meydana gelir. Bu tür kümeler, kayma dalgası ayırma yöntemi kullanılarak kabuksal anizotropinin ölçülmesi için uygundur. Bu yüzden, bu deprem kümeleri, bu bölgenin altındaki kabuksal anizotropinin ölçülmesini mümkün kılmıştır. Ayrıca, sismik anizotropi ile sismik b değeri arasındaki olası bir ilişkinin olup olmadığını bulmak için depremlerin frekans-büyüklük ilişkisi mekânın bir fonksiyonu olarak kullanılarak sismik b değeri ve stres değerleri hesaplanmıştır. Sismik b-değeri için, 1 Ocak 2010 – 28 Şubat 2019 arasında 1,0'den büyük olan KOERI (Boğaziçi Üniversitesi, Kandilli Rasathanesi ve Deprem Araştırma Enstitüsü, Bölgesel Deprem-Tsunami İzleme Merkezi) tarafından hazırlanan bir deprem kataloğu kullanılmıştır. Bu nedenle, analizlerden elde edilen bulguların güvenilirliği artırılmıştır çünkü bu bölge için 2010 öncesi depremlerin yer parametrelerinin doğru olarak belirlenmesi, sismik istasyon kapsamı eksikliği nedeniyle güvenilir değildir. Ayrımlanma analizi için bu bölgede 2016'dan 2017'ye kadar meydana gelen mikro depremler ilk olarak seçilmiştir. Kayma dalgası bölme analizinden elde edilen sonuçlar ayrımlanma parametrelerinde güçlü saçılma olduğunu göstermiştir. Bu gözlem deprem sürülerinin neden olduğu stres birikimi ile tutarlı görünmektedir. Ayrıca, stresteki farklılıklar nedeniyle, her istasyon için ortalama zaman gecikmesinde değişiklikler gözlenmiştir. Çalışmanın bir diğer önemli gözlemi, kayma dalgası polarizasyonlarının 90 °'lik saçılımdır. Sismik olarak aktif fay düzlemlerinde dalgalı yüksek gözenekli sıvı basınçları, kayma dalgası bölme parametrelerinde saçılma modelinin en muhtemel nedenidir.

Anahtar Kelimeler: *Simav, sismik anizotropi, kayma dalgası ayrımlanması, stres, b değeri, sismik tehlike.*

Introduction

In recent years, shear wave splitting is widely used in seismological studies to reveal localized anisotropy within the Earth. Particularly, it efficiently provides a powerful diagnostic of mantle anisotropy (e.g., Silver and Chan, 1991; Savage, 1999; Lynner and Long, 2014; Agius and Lebedev, 2017). In addition, this method is used to investigate crustal anisotropy using micro earthquakes (e.g., Crampin, 1981; Nishizawa, 1982; Peacock and Hudson, 1990; Crampin et al., 2008; Polat et al., 2012). The studies indicated that the presence of preferably oriented structures in the crust such as layers, parallel aligned fractures, cracks, micro-cracks or the presence of minerals with a preferred orientation in rocks primarily cause seismic crustal anisotropy. Investigating seismic anisotropy provides to get information about the deformation, stress and faulting of the crust. Therefore, to measure seismic anisotropy within the earth, shear wave splitting is generally used as a common tool because it is a clear indicator of anisotropic structure of the earth and is generally unaffected by

isotropic wave speed heterogeneity (e.g., Silver, 1996; Savage, 1999; Long and Silver, 2009). The shear wave splitting parameters (fast polarization direction ϕ and delay time δt) give us valuable information about the orientation of the stress, crack geometry and crack density (e.g., Crampin, 1994). The widely observed shear-wave splitting (SWS) (seismic bi-refringence) in the Earth's crust, is caused by propagation through the anisotropic geometry of the stress-aligned fluid-saturated micro-cracks pervading most crustal rocks (Crampin, 1994; Crampin and Gao, 2013). The widespread SWS above swarms of small earthquakes in Iceland and elsewhere (Crampin, 1994; Crampin and Peacock, 2008; Crampin et al., 2008) indicate that micro-cracks are pervasive throughout the Earth's crust. Since micro-crack geometry is sensitive to variations in stress, changes in SWS can be interpreted in terms of variations of the in situ-stress in the rock mass surrounding the swarm. This allows stress-accumulation before earthquakes to be recognized and earthquakes stress-forecast (Crampin et al., 1999, 2008; Crampin and Gao, 2013). Note that for this particular application, it was preferred the term earthquake stress-forecast to earthquake prediction. Monitoring SWS above a persistent swarm in SW Iceland associated with transform zones of the Mid-Atlantic Ridge, where they run onshore in SW and N Iceland, allowed stress-accumulation before a M=5 earthquake to be recognized three days before it occurred and the earthquake successfully stress-forecast (Crampin et al., 1999, 2008). Similar effects have been seen retrospectively before some 15 other earthquakes worldwide (Crampin et al., 2015). This near universal SWS implies that most in situ rocks are so heavily micro-cracked that they verge on fracturing and are critical-systems leading to failure in earthquakes if there is any disturbance (Crampin and Gao, 2013). Monitoring such changes in SWS requires recording above persistent swarms of small earthquakes in the shear-wave window with angles of incidence less than ~35º (for typical Poisson's ratios) avoiding interference with S-to-P converted phases (Booth and Crampin, 1985).

Although such consistent earthquake swarms located in the Simav region seem consistent to detect crustal anisotropy beneath the study area, it is not easy to determine correctly starting and ending points of S phases on the waveforms of small earthquake because of the complexity of the shear-wave signal (Crampin and Gao, 2006). Before splitting analysis, in this study, seismic b-value and stress were investigated by using the frequency–magnitude relationship of earthquakes as a function of space. As a first in this study, the obtained results from these analyses were combined to find out whether there is a possible relationship between seismic anisotropy and seismic b-value (Changhui, et al., 2019).

Tectonics and seismicity of the Simav region

The Simav region is located in the western part of Turkey and was formed by extensional tectonic regime (Figure 1). As seen in Figure 1, Gediz, Emet and Simav Fault Zones are the main tectonic structures in this region. Kocyigit (1984) shows that continuous tectonic movements in Simav and surrounding regions are highly deformed but graben and basin systems in these regions are fairly formed (see Figure 1). Koçyiğit (1984) also demonstrated that active faulting can be seen in different geologic formations. Shaded regions indicated in Figure 1 represent Quaternary alluviums. One of the recent studies carried out by Gündoğdu et al. (2017) aimed to determine the Late Cenozoic geodynamic evolution of Simav by using datations of the active tectonic structures in the region (Simav Fault and Simav Detachment Fault) and granitic and volcanic rocks of the Eğrigöz Magmatic Complex. This study indicated that the Simav Fault that displayed previously a strike-slip character currently has listric normal fault behavior after a tectonic regime change in the Plio-Quaternary. Also, there was observed a transition from compressional regime to a regional extensional regime. They suggested that the cause of the tectonic regime change is related to the complex subduction process (slab-pull and rollback) between the African Plate and Anatolian Plate in the Eastern Mediterranean.

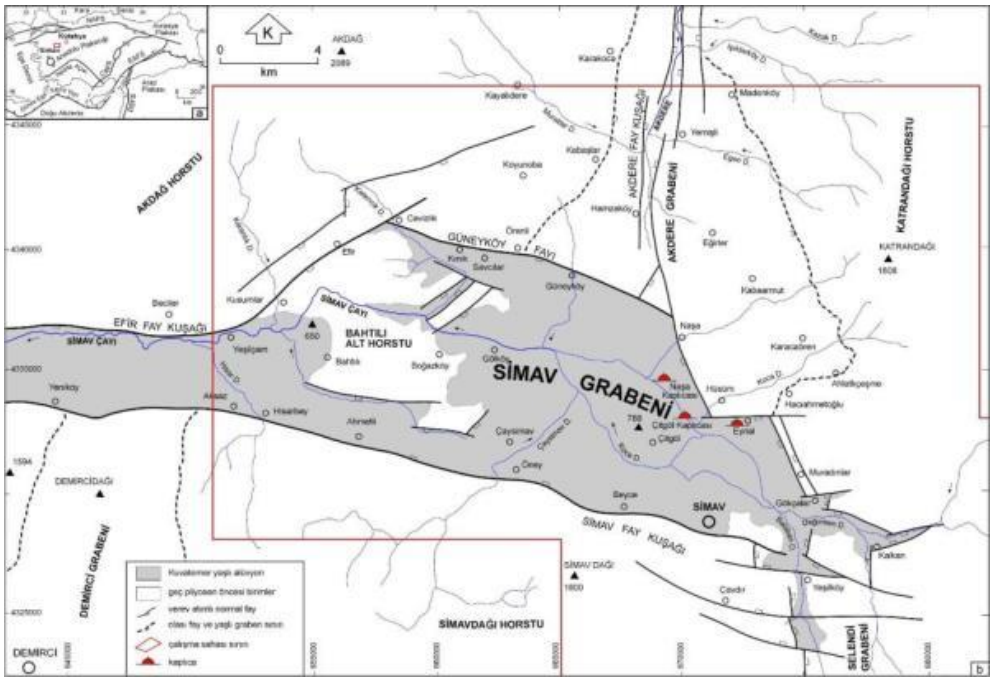


Figure 1. Detailed tectonic features of the study area (modified from Koçyiğit, 1984).
Şekil 1. Çalışma alanının detaylı tektonik özellikleri (Koçyiğit, 1984'ten değiştirilmiş.)

Throughout history, many devastating earthquakes often occurred in this region. The historical earthquakes occurred in this region before the instrumental period were listed in

Table 1. The dates, intensities and locations of the seismic events given in Table 1 were obtained from the AFAD (Republic of Turkey Prime Ministry Disaster and Emergency Management Authority Presidential of Earthquake Department) (Deprem, 2019 deprem.gov.tr). In addition to this, earthquakes from 1900 to present with magnitude greater than 5 were shown in Figure 2. During this period, 117 intermediate and devastating earthquakes occurred in the study area. This gives significant information about that it is possible for a hazardous earthquake to occur in this region. As listed in Table 1, the intensities of the unrecorded events were also very high. These earthquakes indicate that the Alaşehir-Simav Fault system causes devastating earthquakes due to the fact that it is an active tectonic zone. The largest event occurred in Dinar in 1875 according to the AFAD catalog. Prominently, the 1875 earthquake resulted in a death toll of 1300 in a region between Çivril and Dinar provinces (Oncel et al., 1998). A 20-km long rupture zone was observed (Pınar and Lahn, 1952; Ambraseys, 1975). This table also indicated that there are no earthquakes between 94-1766 years, possibly related to a seismic gap or quiescence of seismicity. Furthermore, in February 17, 2009 an earthquake with a ML=5.0 occurred in the region. Intermediate earthquakes can be expected for this region because it is seismically very active.

Table.1 Historical earthquakes occurred on the Alaşehir-Simav fault system (acquired from Deprem, 2019).
Çizelge 1. Alaşehir-Simav fay sisteminde meydana gelen tarihsel depremler (Deprem, 2019'dan alınmıştır).

Date	Location	Intensity
B.C.88	Dinar	Unknown
53	Dinar and its surroundings	VIII
94	Afyonkarahisar and its surroundings	VIII
1766	Şuhut	VIII
1795	Afyonkarahisar	VIII
1862	Afyonkarahisar and Şuhut	VIII
1873	Afyonkarahisar	VI
03.05.1875	Dinar and Çivril	IX
13.05.1876	Afyonkarahisar	VI

Also, the instrumental records indicated that the Emet earthquake with M 6.2 occurred in western Turkey in 1928. In addition to this event, on March 28, 1970, the Gediz earthquake with Mw 7.2 occurred in this region. The 1970 Çavdarhisar earthquake with M 5.9 can be considered as an other important event occurring in this region. In February 17, 2009 an earthquake with a ML=5.0 occurred in the region. Intermediate earthquakes can be expected for this region because it is seismically very active. Also, the instrumental records indicated

that, in March 28, 1970 Gediz earthquake with Mw 7.2 occurred in the region. In addition to this event, 1928 Emet earthquake M 6.2 and 1970 Çavdarhisar earthquake M5.9 can be considered as other important events occurring in this region (Oncel et al., 1998). To get information about the seismicity of the region, earthquakes with magnitude greater than 5 from 1900 to 28 February 2019 and greater than 1 from 1 January 2010 to 28 February 2019, were together indicated in Figure 2.

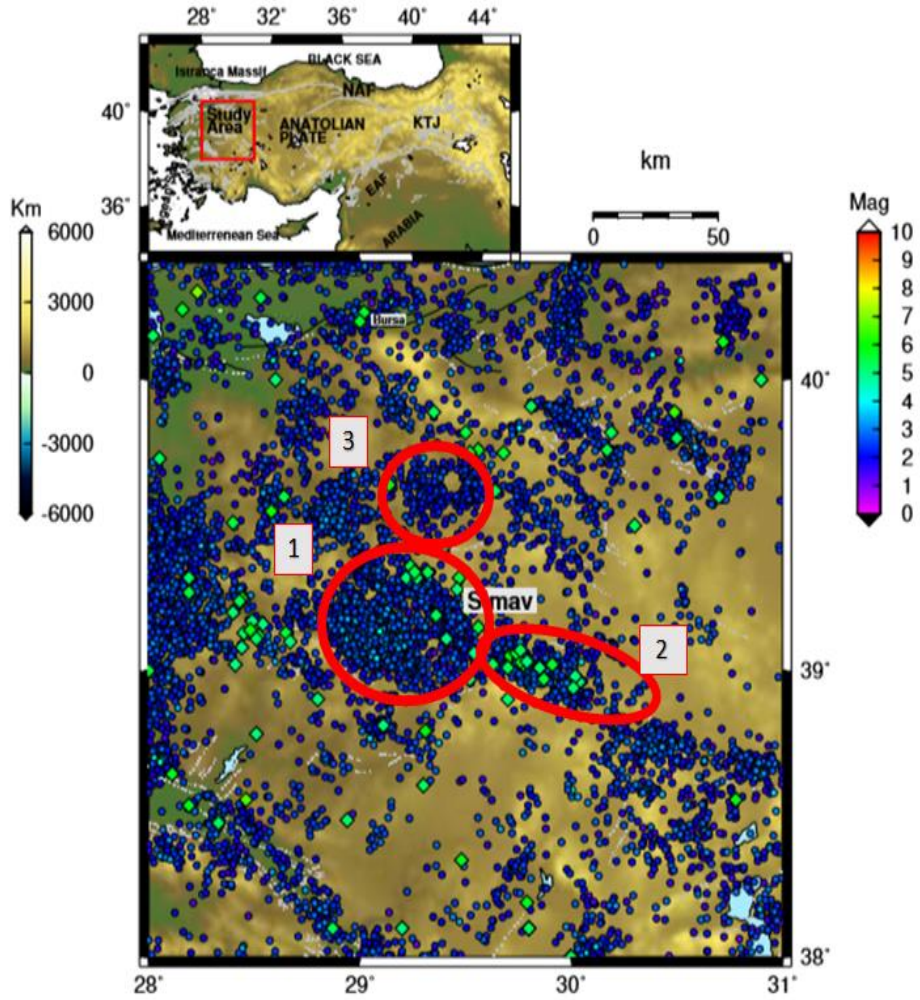


Figure 2. Tectonic map of the Simav region (dot gray faults from Saroglu, 1987). Inset: The location of the study area within Turkey is marked red. (KTJ) Karlıova Triple Junction; (EAF) East Anatolian Fault and (NAF) North Anatolian Fault. Green circles show earthquakes with magnitude greater than 5 from 1900 to 2019 occurred in this study area. Earthquakes from 1 January 2010 to 28 February 2019 with magnitude greater than 1 from were colored according to event magnitude.

Şekil 2. Simav bölgesinin tektonik haritası (Gri faylar Saroğlu, 1987'den alınmıştır). İçindekiler: Çalışma alanının yeri Türkiye içinde kırmızı olarak işaretlenmiştir. (KTJ) Karlıova Üçlü Kavşağı; (EAF) Doğu Anadolu Fayı ve (NAF) Kuzey Anadolu Fayı. Yeşil daireler bu çalışma alanında 1900'den 2019'a kadar 5'ten büyük depremler göstermektedir. 1 Ocak 2010 - 28 Şubat 2019 tarihleri arasında 1'den büyük depremler, deprem büyüklüğüne göre renklendirilmiştir.

Data and Methods

The earthquake catalog prepared by Boğaziçi University, Kandilli Observatory and Earthquake Research Institute, Regional Earthquake-Tsunami Monitoring Center (Kandilli Observatory and Earthquake Research Institute of Boğaziçi University, Kandilli (2019)) was used to calculate a-value, b-value and Mc (Magnitude of Completeness). A well-known empirical relation in earthquake seismology is the Gutenberg–Richter relation. The empirical relation represents the frequency of occurrence of earthquakes as a function of magnitude. The constants of the empirical relation are comprised of the a-value and b-value. The a-value is related to the seismic activity. The b-value (size distribution) is a measure for the relative abundance of the strong to the weak earthquakes. In other words, the b-value gives information about the earthquake occurrence probability (Godano et al., 2014). Therefore, the b-value can be said to be related to the tectonic regime of the investigated area.

The location of seismic stations is shown in Figure 3. The coverage of stations deployed in this region seems fine after 2010, but it is not enough to accurately determine the location parameters of micro earthquakes with magnitude less than 1 (more information about the installation dates of receivers installed in this region is available at http://www.koeri.boun.edu.tr/sismo/2/tr/). The catalog consists of earthquakes occurred in this area between the latitudes of 38°- 40.4° and the longitudes of 28°- 31°. In this area, approximately 14757 micro earthquakes with magnitude equal or greater than 1 occurred between 2010 and 28 February 2019 were selected (Figure 2). Before 2010, the location parameters of the events are not reliable because of lack of coverage of seismic stations as seen in Figure 3. Before this time, the intermediate and destructive earthquakes occurred in this study area were not considered in this study. In addition, the catalog did not include events with magnitude less than 1. To check the earthquake catalog, the time dependent variation and compliance for sub-regions were also analyzed. To make a detailed comparison, the studied region was divided into three sub-regions shown in Figure 2 according to earthquake clusters and active faults located in this region (shown in Figure 1). To visualize the results of calculation of cumulative number and Frequency-Magnitude Distribution (FMD) of the seismic events, ZMAP software was used (Gutenberg and Richter, 1944; Wyss et al., 2001). The Gutenberg–Richter relation (Gutenberg and Richter, 1944), one of the well-known empirical relation between frequency and magnitude equation (eq. 3.1) is usually applied in the modeling of the seismic hazard, and is related to the earthquake precursors and probabilistic seismic risk assessments (Jarahi, 2017). This approach presents the frequency of occurrence of earthquakes as a function of magnitude (Eq. 3.1):

$$\log_{10}N = a - bM \qquad \text{(Eq. 3. 1)}$$

In this equation, N represents the cumulative number of earthquakes with magnitude greater than M where a-value and b-value are constants to be determined. The a-value and b-value constants are related to seismic activity and distribution of magnitude size, respectively.

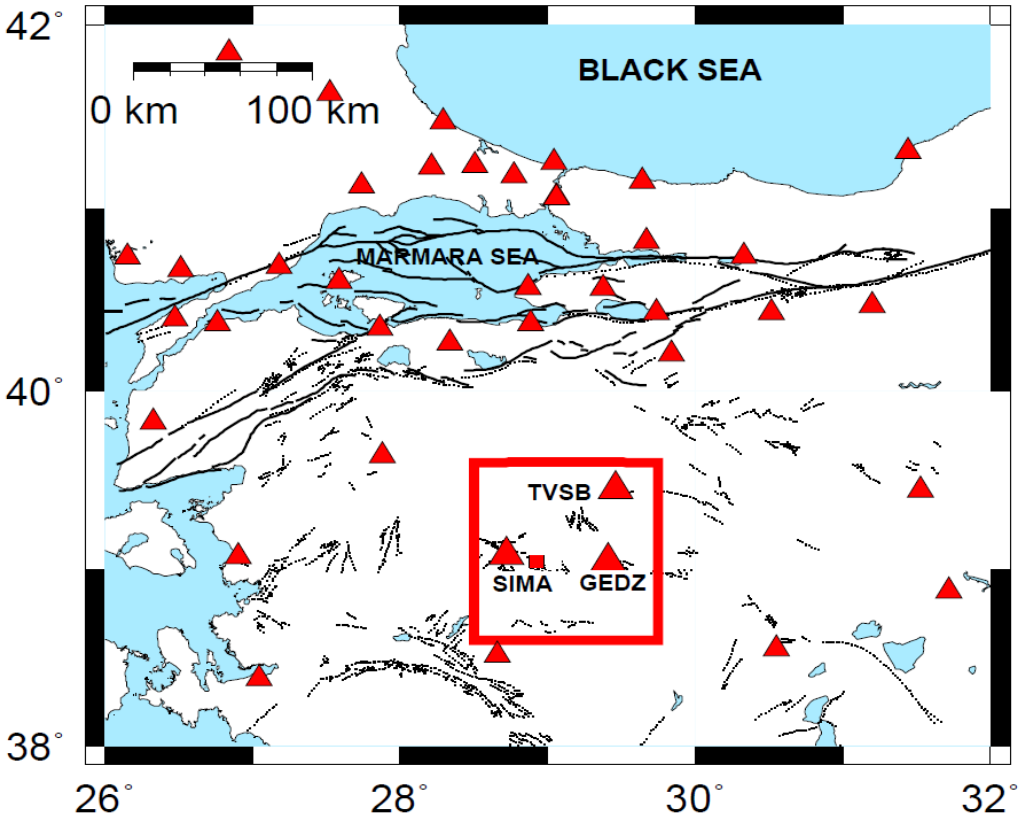


Figure 3. Distribution of seismic stations located in the study region.
Şekil 3. Çalışma bölgesinde bulunan sismik istasyonların dağılımı.

Several studies revealed spatial variations in the frequency-magnitude distribution in different tectonic regimes (Wyss et al., 1997; Wiemer and Wyss, 1997). There are some studies that spatial and temporal changes in b-values were detected prior to large earthquakes (Murase, 2004; Nakaya, 2006). Some studies (Mogi, 1962; Warren and Latham, 1970) indicated that changes in the b-values may be caused by material heterogeneity and thermal gradient. To explain the temporal and spatial earthquake activities in a region in different scales, this approach may be used.

Before using ZMAP software (Weimer, 2001), to construct a homogenous catalog, the Md magnitude of the complete dataset was converted to ML magnitude by using the following equation (Kalafat, 2016):

$$ML=(0.9897*Md)+0.0978 \quad (\text{Eq.3.2})$$

In addition to this, to remove duplicated events in the used catalog, the catalog was declustered by Reasenberg (1985) and Gruenthal algorithm (detail information about this algorithm is available in Weimer (2001)). Before and after the declustring procedures, Mc (Magnitude of Completeness), b-value, a value and annual from the declustered data's analyses are .6, 1.51-/+0.03, 8.165, 7.663, 2.6, 1.88-/+0.03, 8.444 and 7.489, respectively (see the left and right sides of Figure 4). Before and after declustring the catalog, Mc does not change, but there is a noticeable change between b values. The study region was additionally divided into three sub-regions to compare b and Mc values for each region (Figure 2). Mc for region 1 and region 3 is 2.7. Although both regions have same Mc value, their b values are different from each other. Their b values for each region are 1.47-/+0.02 and 1.6-/+0.08, respectively. On the other hand, Mc value is 2.6 for region 2.

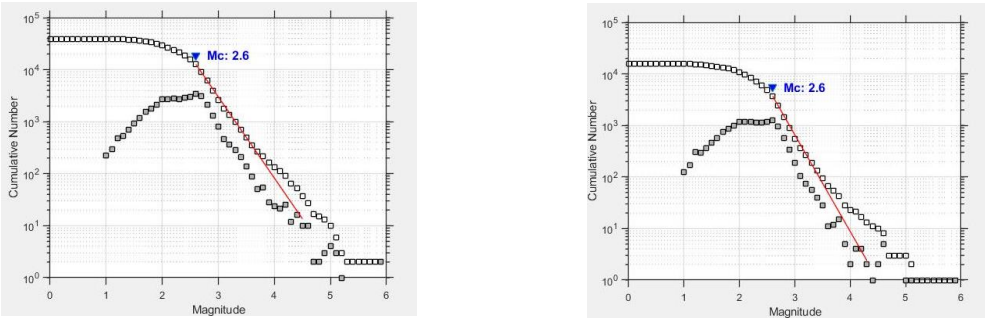


Figure 4. Frequency-Magnitude Distribution (FMD) from 2010 to 1 January 2019 earthquake catalog. The red thin line represented Gutenberg-Richter equation, log N=a-bM. The left and right figures were produced from raw and declustered catalogs, respectively.

Şekil 4. 2010'dan 1 Ocak 2019'a kadar olan deprem kataloğundan Frekans-Büyüklük Dağılımı (FMD). Kırmızı ince çizgi Gutenberg-Richter denklemini temsil etmektedir, log N = a-bM. Sol ve sağ şekiller sırasıyla ham ve declustered kataloglardan üretildi.

After calculation the Mc, a-value and b-value mentioned above, micro-earthquakes were prepared for SWS analysis. Initially, waveforms of micro-earthquakes from between 01 January 2015 to 05 May 2016 occurring in Simav and surrounding region recorded by seismic stations (Figure 3) operated by KOERI were collected. A total of 600 micro earthquakes (Figure 5) were relocated in study area by using zSacWin (Yılmazer, 2003). The zSacWin (Yılmazer, 2003) was developed as an earthquake processing software for KOERI. This earthquake processing software is based on HYPO71 (Lee and Lahr, 1975). During relocation process, each waveform of the events is visually picked. The data set was constrained by using the following three criteria: (1) the standard error of epicentre and depth is less than or equal to 1 km; (2) the number of phase readings is more than 9; and (3) the rms-value is less than 0.9 s. During analysis of the data, the criteria was certainly considered

to enhance reliability of splitting analysis. In addition, the quality of the recorded three-component waveforms were visually checked and those with bad channels rejected in order to provide good signal-to-noise ratio of the incoming wave and identify more clearly the impulsive nature of the shear-waves on the seismograms. In particular, the depths of the relocated events were expected to be equal or greater than the distance between the recorder and the source to restrict arrivals to the shear-wave window. Due to this, more than 250 events are discarded from the data set. Furthermore, before shear- wave splitting analysis, a Butterword band-pass filter is applied in range from 1 to 10 Hz to improve signal to noise. Also, Figure 5 indicates the approximate locations of earthquakes in a 100 km square around Simav. As seen in Figure 3, there are far too few seismic stations near the SIMAV Swarm either to accurately locate the swarm events or to monitor the behavior of shear-wave splitting within the shear-wave window of seismic station above the swarm events. To acquire primary splitting measurements, initially, incidence angles of events were checked because the waveforms of shear-waves outside an effective window of ~45o can be severely distorted from the polarisations of the incident wave by the effect of S-to-P conversions on shear-wave energy (Crampin and Gao, 2006).

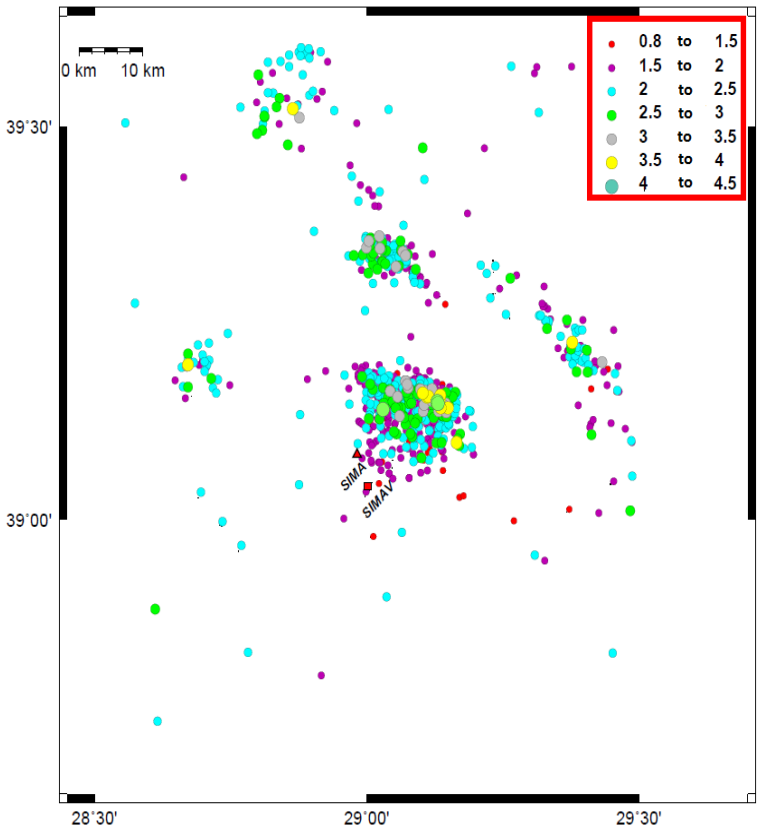


Figure 5. The locations of relocated events (01/01.2015 - 05/05.16) in a 100 km by 100 km square around Simav.

Şekil 5. Tekrar lokasyonu yapılan depremler (01/01.2015 - 05/05.16), Simav çevresinde 10^4 km^2 alan içerisinde yer almaktadır.

To get rid of such a problem, distribution of relocated events within the effective shear-wave window of incidence less than 45° was mapped in Figure 6. After all these preparation steps, the shear-wave phase on seismograms are initially visually checked and then shear wave window was manually determined. To determine splitting parameters, we used the shear wave splitting method based on the Shear-wave Birefringence Analysis (SHEBA) (Wuestefeld et. al., 2003) after Silver and Chan (1991) (Figure 7). In this method, the calculated splitting parameters (Φ - fast polarization direction, and δt - delay time) are sensitive to the choice of the manually selected shear-wave analysis window for the analysis. Time windows of different lengths are visually checked to determine an acceptable window length of the analyzed signals because reliable results, in general, are stable over a range of windows lengths.

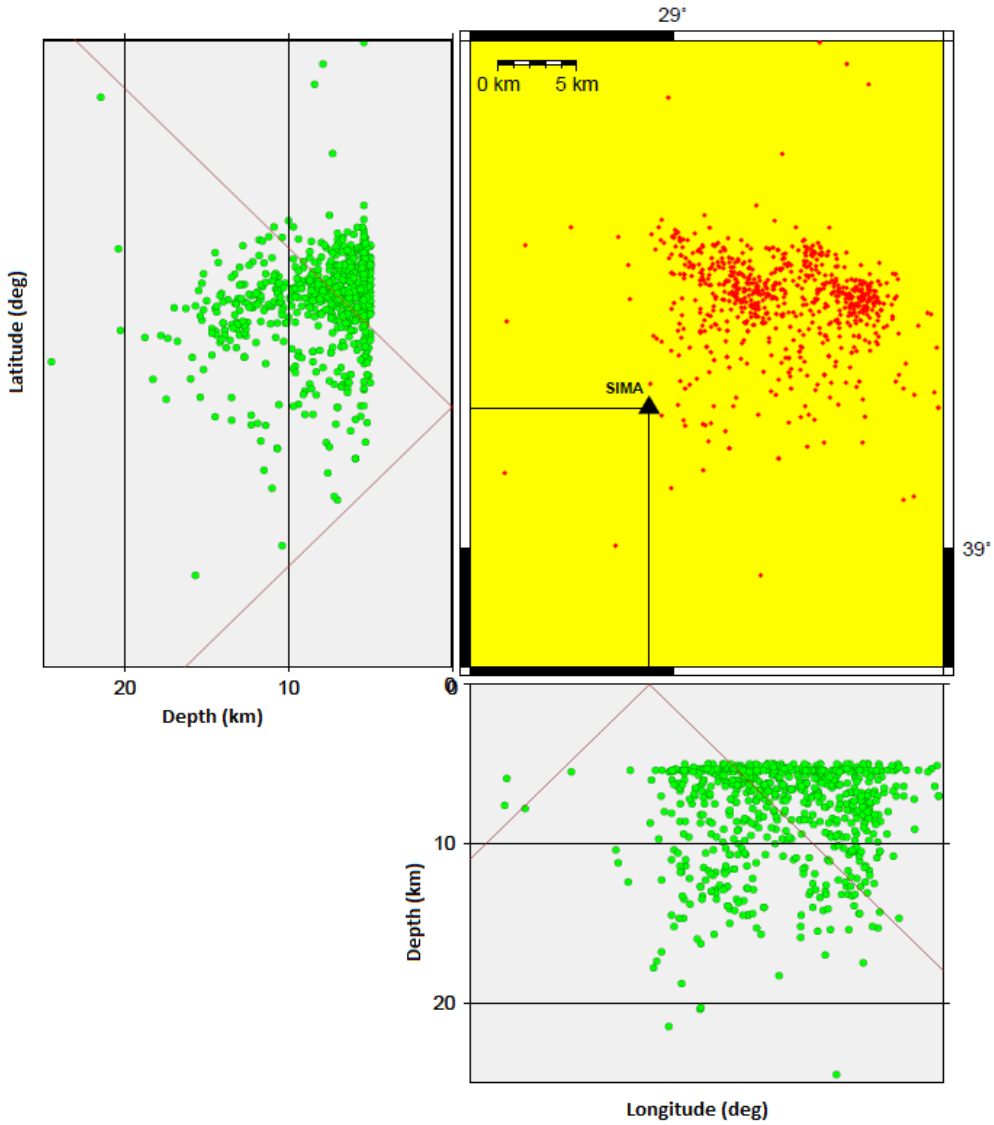


Figure 6. Distribution of relocated events within the effective shear-wave window of incidence less than 45º.

Şekil 6. 45^0 'den az insidans açısının etkili kesme dalgası penceresi içerisinde kalan tekrar lokasyonu yapılan depremlerin dağılımı.

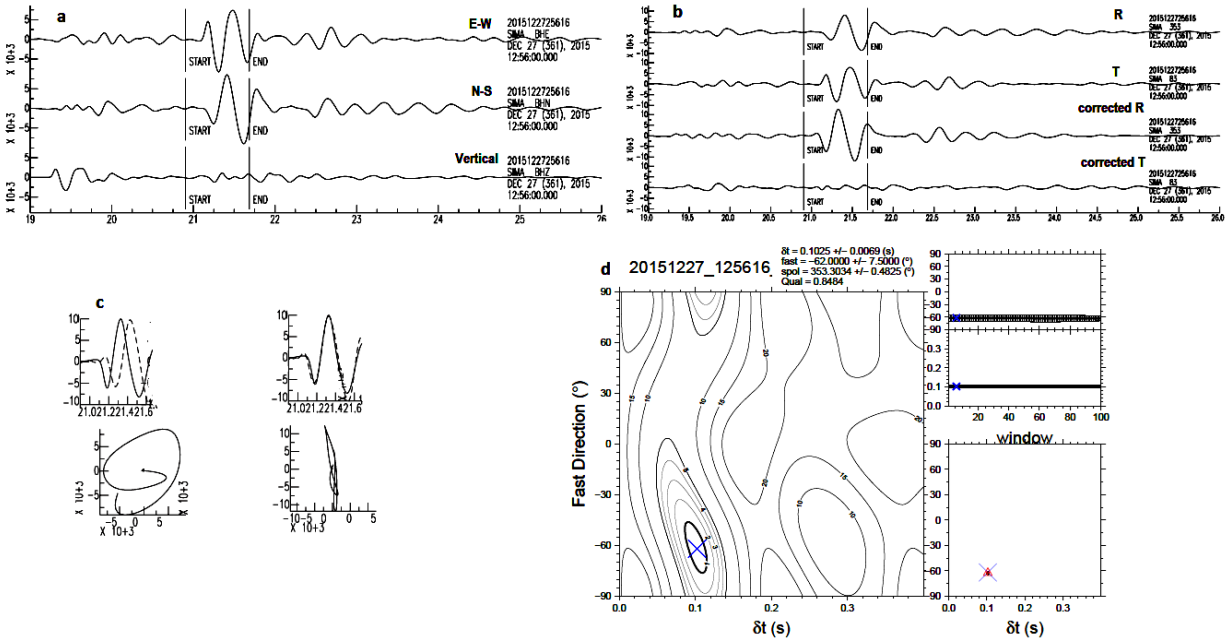


Figure 7. Illustration of SHEBA technique on microseismic data. (a) filtered data rotated into the frame of the ray such that E-W and N-S are perpendicular to the ray path and vertical is along the ray path. (b) Radial and transverse components are obtained. START and END are the beginning and end of the shear-wave analysis window. (d) A grid search over Φ and δt is performed to find the parameters that best linearize the particle motion. The cross shows the solution, and the thick contour is the 95% confidence interval. The labels next to the figure give delay time-δt, Φ-fast direction, and source polarization direction. (b) Radial and transverse components before and after the splitting correction. (c) Fast and slow shear waveforms (top) and particle motion (bottom) before (left) and after (right) the shear wave splitting correction. As seen, the fast and slow waves have similar waveforms, and the particle motion is also linearized after the splitting correction. For that, the energy should be minimized on the corrected transverse component in the shear-wave analysis window.

Şekil 7. Mikrosismik verilerde SHEBA tekniğinin gösterimi. (a) E-W ve N-S'nin ışın yoluna dik ve ışın yolu boyunca düşey olacak şekilde, ışın çerçevesi boyunca filtrelenmiş veriler döndürülmüştür. (b) Radyal ve enine bileşenler elde edilir. BAŞLAT ve SON, kayma dalgası analiz penceresinin başlangıcı ve bitişidir. (d) Parçacık hareketini en iyi şekilde lineer hale getiren parametreleri bulmak için Φ ve δt üzerinde bir ızgara araştırması yapılır. Çarpma işareti çözümü gösterir ve kalın kontur % 95 güven aralığındadır. Şeklin yanındaki etiketler gecikme zamanı δt, Φ hızlı yön ve kaynak polarizasyon yönünü gösterir. (b) Ayrılma düzeltmesinden önce ve sonra radyal ve enine bileşenler. (c) Hızlı ve yavaş kayma dalga formları (üstte) ve parçacık hareketi (altta) kayma dalgası bölme düzeltmesinden önce (solda) ve sonra (sağda). Görüldüğü gibi hızlı ve yavaş dalgalar benzer dalga formlarına sahiptir ve parçacık hareketi de ayrımlanma düzeltmesinden sonra doğrusallaşır. Bunun için, kayma dalgası analiz penceresindeki düzeltilmiş enine bileşende enerji en aza indirilmelidir.

The most reliable results are derived from the determined windows over which the splitting parameters remain stable. The rose diagrams in the roundels are SWS polarizations at monitored station SIMA (Figure 8). The premature polarizations at SIMA are NW-SE in the direction of regional tectonic stress throughout Simav region. The previous geologic and tectonic studies conducted by earth scientists ((e.g., Kocyigit, 1984: Akgun and Ozden, 2019) indicated that the WNW-ESE-trending oblique-slip normal faults strongly influence seismic activity of the region.

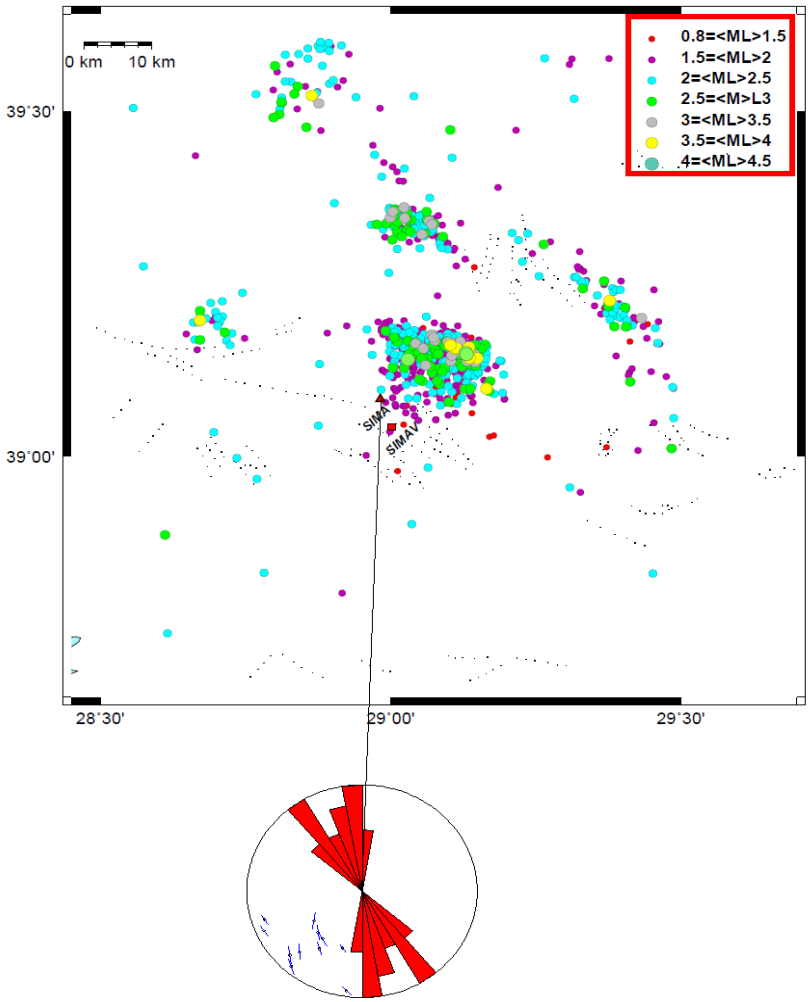


Figure 8. Seismicity map (M ≥ 1) of the Simav region January 2015 to May 2016. The red triangle shows a station SIMA located in the above persistent swarms of small earthquakes associated with the extensional tectonic regime of western Turkey occurred. Roundels are equal-area rose-diagrams of SWS polarizations, obtained from micro-earthquakes from January 2016 to May 2016 occurred in the Simav region, superimposed on equal-area polarizations out to 45º of individual straight-line shear-wave arrivals with length proportional to time-delay.

Şekil 8. Ocak 2015 - Mayıs 2016 tarihleri arasında Simav bölgesindeki sismik harita (M ≥ 1). Kırmızı üçgen, Türkiye'nin batıdaki genişlemeli tektonik rejimi ile ilişkili küçük deprem sürülerinde yer alan bölgedeki SIMA istasyonunu göstermektedir. Çemberler, SWS polarizasyonlarının eşit alanlı gül diyagramlarıdır: Ocak 2016-Mayıs 2016 arasında Simav bölgesinde meydana gelen mikro depremlerden elde edilen, uzunlukları gecikme süreleri ile orantılı olarak 45º dışındaki bireysel düz hatttaki kesme dalgası varışlarının eşit alan polarizasyonlarına bindirilmiş halidir.

All seismically active faults are generally enveloped by critically high-pressure pore fluids that relieve stress perpendicular to the faults and allow faults to slip (Crampin et al., 1999, 2002, 2003; Volti Crampin, 2003a, 2003b). However, in our case, shear-wave polarizations are parallel to the strike of the fault (Crampin et al., 2002) because such critically-high pore-pressures cause 90°-flips in shear-wave polarizations (Angerer et al., 2002) for shear waves propagating close to the fault. In the next study, as a future work, the seismic data recorded by the rest of stations deployed in this region will be analyzed by using SWS method.

DISCUSSION

Crampin and Gao (2013) analyzed micro- earthquakes associated with transform zones of the Mid-Atlantic Ridge where they run onshore in SW and N Iceland to monitor variations in stress before and after impending strong earthquake with shear-wave splitting. These persistent swarms have been used as the source of shear-waves for monitoring changes in shear-wave splitting throughout the rock mass surrounding the swarms. Previously thought to be unique, a another persistent swarm is here identified at Simav, ~250 km south of Istanbul in Western Turkey associated with a geothermal hotspot. Western Turkey is much more seismically active than Iceland and the Simav swarm is expected to respond to stress-accumulation before many more large earthquakes than the swarms in SW and N Iceland. However, as of April 2017, there are far too few seismic stations near the SIMAV Swarm either to accurately locate the swarm events or to monitor the behavior of shear-wave splitting within the shear wave window of seismic station above the swarm events. Further analysis must await improved station coverage. The seismicity of Western Turkey indicates a very active role for the Anatolia Plate related to the structure of grabens and basins. A strong persistent swarm has been identified immediately NE of Simav, ~250 km south of Istanbul in Western Turkey (Figure 2) associated with a geothermal hotspot. Western Turkey is much more seismically active than Iceland and the Simav Swarm is expected to respond to stress-accumulation before many more large earthquakes than the swarms in Iceland, and is likely to be a valuable source for studies of shear-waves and shear-wave splitting for stress-forecasting earthquakes in Western Turkey including any threatening Istanbul. Shear wave splitting results revealed a strong scattering in delay time in the 2016–2017 period and a significant variation in the fast shear wave polarization in this time period. Generally, all seismically active faults are enveloped by critically high-pressure pore fluids that relieve stress perpendicular to the faults and allow faults to slip (Crampin et al., 1999, 2003; Volti and Crampin, 2003a, 2003b). However, this study indicated that shear-wave polarizations are parallel to the strike of the fault (Crampin et al., 2002) because such critically-high pore-pressures cause 90º-flips in shear-wave polarizations (Angerer et al., 2002) for shear waves propagating close to the fault. These findings from the study was similar to the previous splitting study carried out in the Marmara region by Polat et al. (2012). This preliminary observation should be provided with more data analyzed by shear wave splitting method. The rose diagrams in the roundels are SWS polarizations at monitored only station SIMA (Figure 6). Rest of data of other stations and station SIMA will be analyzed again. The premature polarizations at SIMA are NW-SE in the direction of regional tectonic stress throughout Simav region. The WNW-ESE-trending oblique-slip normal faults strongly influence the seismic activity of the region (e.g., Kocyigit, 1984; Akgun and Ozden, 2019).

In addition, the Simav graben produced by the latest products of North-South extensional tectonics began in the latest Oligocene-early Miocene times (Seyitoğlu, 1997) influence stress regime observed in the study area because above persistent swarms of small earthquakes associated with the extensional tectonic regime of western Turkey. Roundels are equal-area rose-diagrams of SWS polarizations superimposed on equal-area polarizations out to 45º of individual straight-line shear-wave arrivals with length proportional to time-delay. Due to the results of the ongoing study, finally it can be said that the observed NW-SE fast polarization direction is quite consistent with the neotectonic structure of the study area where is mainly characterized by the N-S extension and E-W trending graben-horst systems bounded by active normal faults. This study also indicated that Mc, b-value and a-value remarkably changes spatially. Although any strong relationship between b-value and seismic anisotropy is not yet revealed for this study, there was a relation between anisotropy and b-value that was revealed (e.g., Araragi et al., 2015; Pastori et al., 2019). In addition, to make a relation between b-value and splitting parameters and more information about the Mc, b-value and a-value, the catalog should be improved with a highly reliable dataset. This significantly implies that an improved and high-quality dataset is required to make possible to make a further and reliable interpretation of the region.

CONCLUSION

The seismic activity of the Simav region is very high so that swarm earthquakes usually occur in this region. Such swarms were usually convenient to measure crustal anisotropy by using shear wave splitting method. The swarms may thus make possible to measure crustal anisotropy beneath the area under consideration. As first, in this study, seismic b-value and stress were investigated by using the frequency–magnitude relationship of earthquakes as a function of space in order to find out whether a possible relation between seismic anisotropy and seismic b-value is or not. Results from shear wave splitting analysis indicated strong scattering in splitting parameters. This observation seems to be consistent with stress accumulation caused by the earthquake swarms. Additionally, due to variations in stresses, changes in the average time-delay for each station were observed. Another important observation of the study is that 90°-flips in shear-wave polarizations observed. Fluctuating high pore-fluid pressures on seismically active fault planes are the most likely cause of the scattering pattern in shear-wave splitting parameters. It was clearly observed that the b-values changed as a function of space because the b-value is very sensitive to large earthquakes and the spatial variation of the aftershocks (Jafari, 2008). Although these important findings from the study were acquired, a strong relationship between b-value and

seismic anisotropy is not observed in this study. This suggests that b-value and seismic anisotropy should be investigated as a function of time before devastating earthquakes, and after aftershocks in order to reveal a possible relationship between them.

ACKNOWLEDGEMENTS

I would like to thank all staffs from KOERI for providing data. Some figures in the paper were created using the GMT software package (Wessel et al., 2013).

REFERENCES

Agius, M.R., Lebedev, S., 2017. Complex, multilayered azimuthal anisotropy beneath Tibet: evidence for co-existing channel flow and pure-shear crustal thickening. Geophysical Journal International, 210(3), 1823–1844.

Akgün E., Özden S., 2019. Plio-Quaternary stress states along the Kütahya Fault and surroundings, NW Turkey. Turkish Journal of Earth Sciences, vol.28, pp.671-686.

Ambraseys, N. N.,1975. Studies in historical seismicity and tectonics. Geodynamics today, 7.

Angerer E, Crampin S, Li X-Y, Davis TL., 2002. Processing, modelling, and predicting time-lapse effects of over pressured fluid-injection in a fractured reservoir. Geophys. J. Int., 149, 267-280.

Araragi, K. R., Savage, M. K., Ohminato, T., Aoki, Y., 2015. Seismic anisotropy of the upper crust around Mount Fuji, Japan. Journal of Geophysical Research: Solid Earth, 120, 2739– 2751. https://doi.org/10.1002/2014JB011554.

Booth, D. C., Crampin, S., 1985. Shear-wave polarizations on a curved wavefront at an isotropic free surface. Geophysical Journal International, 83(1), 31-45.

Changhui Ju, Junmeng Zhao, Ning Huang, Qiang Xu, Hongbing Liu, 2019. Seismic anisotropy of the crust and upper mantle beneath western Tibet revealed by shear wave splitting measurements. Geophysical Journal International, Volume 216, Issue 1, January 2019, Pages 535–544, https://doi.org/10.1093/gji/ggy448.

Crampin, S., 1981. A review of wave motion in anisotropic and cracked elastic-media. Wave Motion 3,343–391.

Crampin S., 1994.The fracture criticality of crustal rocks, Geophys. J. Int., 118, 428-438.

Crampin S, Volti T, Stefánsson R., 1999. A successfully stress-forecast earthquake. Geophys. J. Int., 138, F1-F5.

Crampin S, Volti T, Chastin S, et al., 2002. Indication of high pore-fluid pressures in a seismically-active fault zone [J]. Geophys J Int, 151: F1-F2.

Crampin, S., Chastin, S., Gao, Y., 2003. Shear-wave splitting in a critical crust: III. Preliminary report of multi-variable measurements in active tectonics. Journal of Applied Geophysics, 54(3-4), 265-277.

Crampin, S., Gao, Y., 2006. A review of techniques for measuring shear-wave splitting above small earthquakes. Phys. Earth. Planet. Inter., 159, 1-14.

Crampin S, Gao Y, Peacock S., 2008. Stress-forecasting (not predicting) earthquakes: A paradigm shift ? Geology, 36, 427-430.

Crampin S, Peacock S., 2008. A review of the current understanding of shear-wave splitting and common fallacies in interpretation. Wave Motion, 45, 675-722.

Deprem, 2019. Earthquake database. AFAD Deprem Dairesi Başkanlığı, (Prime Ministry Disaster and Emergency Management Presidency), Ankara. https://deprem.afad.gov.tr/. Accessed on November 2019.

Hatzfeld, D., 2001. Shear wave anisotropy in the upper mantle beneath the Aegean related internal deformation. J. Geophys. Res., 106, 30 737-30 754.

Godano, C., Lippiello, E., L. de Arcangelis, 2014. Variability of the b value in the Gutenberg–Richter distribution. Geophysical Journal International, Volume 199, Issue 3, December, Pages 1765 1771, https://doi.org/10.1093/gji/ggu359.

Gutenberg R., Richter C.F., 1944. Earthquake magnitude, intensity, energy and acceleration. Bull. Seismol. Soc. Am. 32:163–191

Gündoğdu, E., Kurban, Y. C., YALÇINER, C. Ç., Özden, S. , 2017. Simav Fayındaki Düşey Yerdeğiştirmelerin, GPR (Yeraltı Radarı) Yöntemi ile Belirlenmesi. Çanakkale Onsekiz Mart Üniversitesi Fen Bilimleri Enstitüsü Dergisi, 3(2), 17-33.

Jafari, M. A., 2008. The distribution of b-value in different seismic provinces of Iran. In 14th word conference on earthquake engineering (pp. 12-17).

Jarahi, H., 2017. Delineate Location of the Last Earthquake Case Study NW of Iran. American Journal of Geosciences, 17(6).

Kalafat D., 2016. Statistical Evaluation of Turkey Earthquake Data (1900-2015): A Case study. Eastern Anatolian Journal of Science. 2: 14-36

Kandilli, 2019. Earthquake catalog, http://www.koeri.boun.edu.tr/sismo/zeqdb/. Boğaziçi University, Kandilli Observatory and Earthquake Research Institute, Regional Earthquake-Tsunami Monitoring Center (Kandilli Observatory and Earthquake Research Institute of Boğaziçi University. Accessed on November 2019.

Koçyiğit, A., 1984, Güneybatı Türkiye ve yakın dolayında levha içi yeni tektonik gelişim. Türkiye Jeol. Kur. Bült., 27, 1-16.

Lee, W. H. K., Lahr, J. C., 1975. Hypo71 (revised): a computer program for determining hypocenter, magnitude and first motion patter of local earthquakes. Open file report. US Geological Survey, 75.

Lynner, C., Long, M. D., 2014. Testing models of sub-slab anisotropy using a global compilation of source-side shear wave splitting data. Journal of Geophysical Research: Solid Earth, 119(9), 7226-7244.

Mogi, K., 1962. Study of elastic shocks caused by the fracture of heterogeneous materials and its relation to earthquake phenomena. Bull. Earthq. Res. Inst., Univ. Tokyo, 40, 125-173.

Murase, K., 2004. A characteristic change in fractal dimension prior to the 2003 Tokachi-oki earthquake (M J= 8.0), Hokkaido, Northern Japan. Earth, planets and space, 56(3), 401-405.

Nakaya, S., 2006. Spatiotemporal variation in b value within the subducting slab prior to the 2003 Tokachi-oki earthquake (M 8.0), Japan. Journal of Geophysical Research: Solid Earth, 111(B3).

Nishizawa, O., 1982. Seismic velocity anisotropy in a medium containing oriented cracks. Journal of Physics of the Earth, 30(4), 331-347.

Öncel, A., Koral, H., Alptekin, O., 1998. The Dinar Earthquake (Mw = 6.2; October 1, 1995; Afyon-Turkey) and Earthquake Hazard of the Dinar-Çivril Fault, Pure and Applied Geophysics. 152. 91-105, 10.1007/s000240050143.

Pastori, M., Baccheschi, P., Margheriti, L., 2019. Shear wave splitting evidence and relations with stress field and major faults from the “Amatrice-Visso-Norcia Seismic Sequence”. Tectonics.

Peacock, S., Hudson, J. A., 1990. Seismic properties of rocks with distributions of small cracks. Geophysical Journal International, 102(2), 471-484.

Pınar, N., Lahn, E., 1952. Turkish Earthquake Catalog with Descriptions. Technical Report, Turkey The Ministry of Public Works and Settlement, The General Directorate of Construction Affairs, Serial 6, no. 36.

Polat, G., Ozel, N. M., Crampin, S., Ergintav, S., Tan, O., 2012. Shear wave splitting as a proxy for stress forecast of the case of the 2006 Manyas-Kus Golu (Mb= 5.3) earthquake. Natural Hazards and Earth System Science, 12(4), 1073-1084.

Reasenberg, P., 1985. Second-order moment of central California seismicity, 1969-82,J. Geophys. Res.,90, 5479–5495.

Savage, M.K., 1999. Seismic anisotropy and mantle deformation: what have we learned from shear wave splitting? Rev. Geophys., 37, 65-106.

Seyitoğlu, G., 1997. The Simav Graben: An example of young E-W trending structure in the late Cenozoic Extensional system of western Turkey. Trans. J. Earth Sci, 6, 135-141.

Silver, P.G., 1996. Seismic anisotropy beneath the continents: probing the depths of geology. Annu. Rev. Earth Planet. Sci. 24, 385–432.

Silver, P.G., Chan, W. W., 1991, Shear wave splitting and sub-continental mantle deformation. J. Geophys. Res., 96, 16429-16454.

Long, M.D., Silver, P.G., 2009. Shear wave splitting and mantle anisotropy: measurements, interpretations, and new directions. Surv. Geophys., 30, 407-461.

Volti T, Crampin S., 2003a. A four-year study of shear-wave splitting in Iceland: 1. Background and preliminary analysis, in New insights into structural interpretation and modelling. ed. Nieuwland, D.A., Geol. Soc. Lond., Spec. Publ., 212, 117-133.

Volti T, Crampin S., 2003b. A four-year study of shear-wave splitting in Iceland: 2. Temporal changes before earthquakes and volcanic eruptions, in New insights into structural interpretation and modelling. ed. Nieuwland, D.A., Geol. Soc. Lond., Spec. Publ., 212, 135-149.

Warren, N. W., Latham, G. V., 1970. An experimental study of thermally induced microfracturing and its relation to volcanic seismicity. Journal of Geophysical Research, 75(23), 4455-4464.

Wessel, P., W. H. F. Smith, R. Scharroo, J. F. Luis, F. Wobbe, 2013. Generic Mapping Tools: Improved version released, EOS Trans. AGU, 94, 409-410.

Wiemer, S., Wyss, M., 1997. Mapping the frequency-magnitude distribution in asperities: An improved technique to calculate recurrence times? Journal of Geophysical Research: Solid Earth, 102(B7), 15115-15128.

Wuestefeld, A., Al-Harrasi, O., Verdon, J. P., Wookey, J., Kendall, J.- M., 2010. A strategy for automated analysis of passive microseismic data to image seismic anisotropy and fracture characteristics, Geophysical Prospecting, 58(5), 753–771, doi:10.1111/j.1365-2478.2010.00891.x.

Wyss, M., Shimazaki, K., Wiemer, S., 1997. Mapping active magma chambers by b values beneath the off-Ito volcano, Japan. Journal of Geophysical Research: Solid Earth, 102(B9), 20413-20422.

Wyss, C., Giannella, C., Robertson, E., 2001, September. Fastfds: A heuristic-driven, depth-first algorithm for mining functional dependencies from relation instances extended abstract. In International Conference on Data Warehousing and Knowledge Discovery (pp. 101-110). Springer, Berlin, Heidelberg.

WIEMER, S., 2001. A software package to analyze seismicity: ZMAP. Seismol. Res. Lett. 72, p.373– 382.

Yılmazer, M., 2003. zSacWin (Kandilli Earthquake Processing Software) developed for KOERI. http://www.koeri.boun.edu.tr/.